Enhanced nonlinearity by H-bonded polymer–dye complex in liquid crystal for holographic gratings

Elena Ouskova,[1,2,3,*] Andrii Pshenychnyi,[1] Antoni Sánchez-Ferrer,[4] Dariia Lysenko,[1,3] Jaana Vapaavuori,[1,5] and Matti Kaivola[1]

[1]*Department of Applied Physics, Aalto University School of Science, P.O. Box 13500, FI-00076 Aalto, Finland*
[2]*Beam Engineering for Advanced Measurements Company, 809 S. Orlando Ave., Suite I, Winter Park, Florida 32789, USA*
[3]*Institute of Physics, National Academy of Sciences of Ukraine, Pr. Nauki 46, Kyiv 03028, Ukraine*
[4]*ETH Zurich, Department of Health Sciences and Technology, Schmelzbergstrasse 9, LFO, CH-8092 Zürich, Switzerland*
[5]*Department of Chemistry, Université de Montréal, P.O. Box 6128, Downtown Station, Montréal, Québec, H3C 3J7, Canada*
**Corresponding author: ouskova@gmail.com*

Received March 24, 2014; revised May 2, 2014; accepted May 3, 2014;
posted May 6, 2014 (Doc. ID 208752); published June 5, 2014

We have studied a new heterogeneous liquid-crystalline material where H-bonded polymer–azo-dye complexes are used as dopants to the liquid crystal (LC) bulk at a very low concentration. Double enhancement of the holographic gratings' diffraction efficiency occurred in the complex-doped LC compared to dye-doped LC. The grating formation/relaxation processes in complex-doped LC showed anomalies that were explained by the presence of polymer with H bonds. The gratings appeared to be formed due to a change of both the absorption coefficient and refractive index. Using such complexes as dopants gives perspectives for tuning and control of the LC properties, and for possible optical applications.

OCIS codes: (160.3710) Liquid crystals; (160.5335) Photosensitive materials; (160.5470) Polymers; (190.4400) Nonlinear optics, materials; (190.4710) Optical nonlinearities in organic materials.
http://dx.doi.org/10.1364/JOSAB.31.001456

1. INTRODUCTION

Azo dyes are popular as dopants to liquid crystals (LCs). They can modify the unique LC properties due to light-induced conformational changes in the azo dye molecules that induce either reorientation of the nematic director or a change in the order parameter. These two parameter changes allow for tuning the LC optical properties in the visible spectrum range and control of light beam propagation. Both conformational [1], supra [2], dye-assisted orientational [3,4], and colossal [5,6] optical nonlinearities have been reported at low light power in comparison with pure LC.

Most of the numerous publications about light-induced effects in azo-doped LCs relate to studies of low-molecular-weight dopants, and extensive experimental data are collected for such systems. Much less work is devoted to studies of LCs doped with azo-containing macromolecular additives [7–10]. Nevertheless, replacement of low-molecular-weight azo dyes with compounds having more complex structures (such as azo polymers or even comb-shaped polymers, carbosilane dendrimers) promises new interesting nonlinear optical effects and potential applications. The studies of nonlinear optical properties of LC with high-molecular-weight dopants have demonstrated their increased optical nonlinearity and peculiarities in their optical response [3,4,7].

Of particular interest are systems based on hydrogen-bonded polymer–azo-dye complexes. Such complexes have the advantage of simple and easy preparation without heavy chemical synthesis, and their components are commercially available. Moreover, H bonding allows modular tunability of the complexes. In our recent studies, we have found that introducing a H-bonded polymer–azo-dye complex into a nematic LC matrix at low concentration results in a self-orientation of the LC in a cell and a spontaneous anchoring transition from planar to homeotropic alignment on a rubbed polyimide surface [8]. Moreover, the unique self-orienting azo compositions showed a strong nonlinear response at very low light powers of cw laser irradiation [9,10]. Self-phase modulation was observed and studied, showing nonthreshold fast formation of aberration rings (on the order of milliseconds) with a change of the refractive index of up to 0.04 and high nonlinear parameter (up to 10^{-3} cm^2/W) at an unusual irradiation geometry: normal incidence of light onto a homeotropically aligned LC. The optical nonlinearity in the complex-doped LC was 1.5 times higher than in an azo-dye-doped LC, and the thermal and conformational mechanisms causing the light-induced order parameter change were suggested [9]. It should be noted that the comparison was made between complex-doped LC and the LC doped with the same azo dye, which was in the complex.

Polymer–azo-dye complex-doped LC looks very promising, as it combines the unique anisotropic properties of LCs with the stability of polymers and the light sensitivity and collective molecular response of azo dyes. The unique properties of LCs doped with hydrogen-bonded polymer–azo-dye complex are determined by a combination of relatively high orientation mobility of the azo fragments and a strong depression of their translation diffusion due to the H bonds. These properties allow us to expect an effective holographic grating recording

to be possible in the LCs doped with hydrogen-bonded complexes. Here, we report on the first observations of dynamic diffraction gratings in such systems.

2. MATERIALS

A classic LC, 4-pentyl-4′-cyanobiphenyl [5CB from PI Chemicals Co., Ltd., Fig. 1(a)], was selected as a nematic matrix for a polymer additive poly(4-vynilpyridine) [P4VP from Polymer Source Inc.; Mn, 1000 g/mol; Mw, 1200 g/mol; Fig. 1(b)]. An azo dye, 4-dimethylamino-4′-hydroxyazobenzene [HAB–DMA from TCI, Fig. 1(c)] formed H bonds with side pyridine fragments of the polymer. The HAB–DMA dye molecule is an azobenzene-type molecule, which absorbs in visible range. As an azo dye, HAB–DMA can undergo *trans*-to-*cis* isomerization that makes it a suitable dopant to trigger light-induced effects in a LC matrix in the visible.

To make the composition, the polymer–azo-dye complex P4VP(HAB–DMA)$_{0.5}$ was prepared by simple mixing of the components in a solvent, as described in detail in [8]. During the formation of the complex, the azo dye statistically connects to every second side fragment of the polymer via H bond, as confirmed with FTIR measurements [11]. We introduced 0.5 wt. % of the complex in 5CB, and the solvent was evaporated. Since the used polymer can be considered oligomeric, the polymer–azo-dye complex is essentially a macromolecular dopant in an LC matrix, and thus it does not disturb LC orientation.

The resulting mixture, 5CB + 0.5%P4VP(HAB–DMA)$_{0.5}$, was studied in a symmetrical cell of 20 μm thickness with planar boundary conditions provided by rubbed polyimide. The doping with the complex led to a slight decrease of the clearing temperature, T_c. The T_c value measured with 0.01°C accuracy in the oriented samples was 35.6°C–35.8°C in pure 5CB and 35.1°C–35.7°C for complex-doped LC.

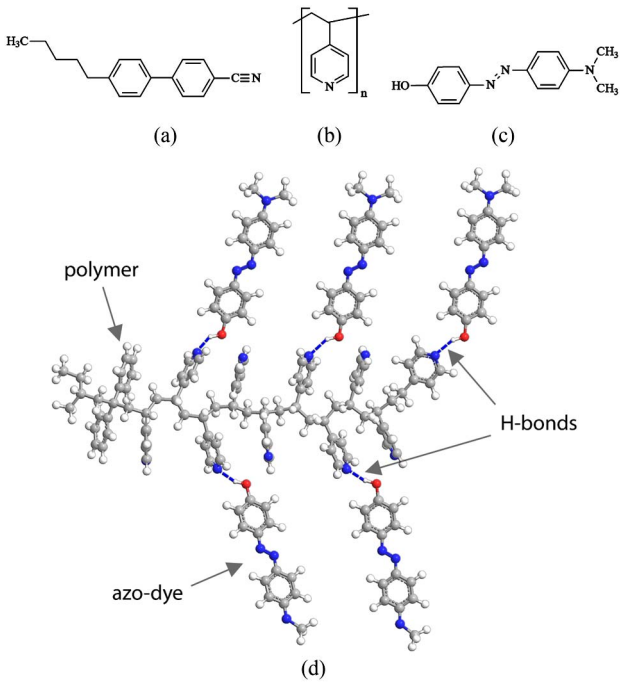

Fig. 1. Chemical structures of (a) the LC 5CB, (b) polymer P4VP, and (c) azo dye (HAB–DMA). (d) 3D sketch of the polymer–azo-dye complex.

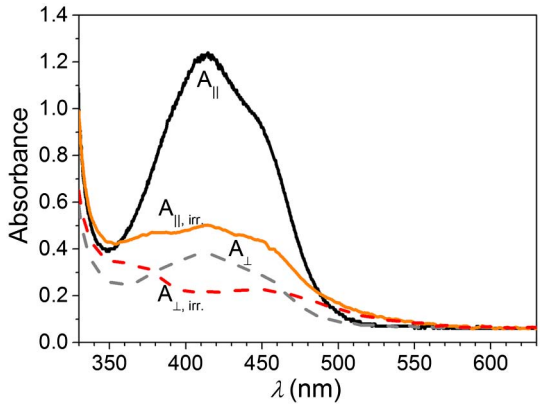

Fig. 2. Polarization absorption spectra of 5CB + 0.5% P4VP (HAB–DMA)$_{0.5}$ before ($A_{\parallel}$ and $A_{\perp}$) and at irradiation ($A_{\parallel,\mathrm{irr.}}$ and $A_{\perp,\mathrm{irr.}}$) with e-wave of 457 nm laser of 300 mW/cm^2. The thickness of the cells was 20 μm.

The polarization absorption spectra of complex-doped 5CB showed two main absorption bands with maxima at $\lambda_{n-\pi^*} = 456$ nm and $\lambda_{n-\pi^*} = 412$ nm (Fig. 2), which appeared to be almost the same as those in azo-dye-doped LC (5CB + 0.25%HAB–DMA) with the same concentration of the dye (0.25 wt. %), with a small shift of the maximum of a few nanometers.

3. EXPERIMENTS

A. Experimental Setup

The nonlinear optical properties of the complex-doped LC were studied by recording the dynamic holographic gratings and comparing the results with LC doped only with the same azo dye at the corresponding concentration. The sinusoidal intensity gratings were recorded by irradiating the cell with two equal linearly polarized beams with a total power $P_0 = P_1 + P_2 = 2P_1$ from an Ar-ion laser ($\lambda_{\mathrm{pump}} = 457$ nm) that intersected at a small angle in the cell's plane (Fig. 3). The incident light wavelength was near the maximum of one of the absorption bands of the mixture $\lambda_{n-\pi^*}$ (see Fig. 2).

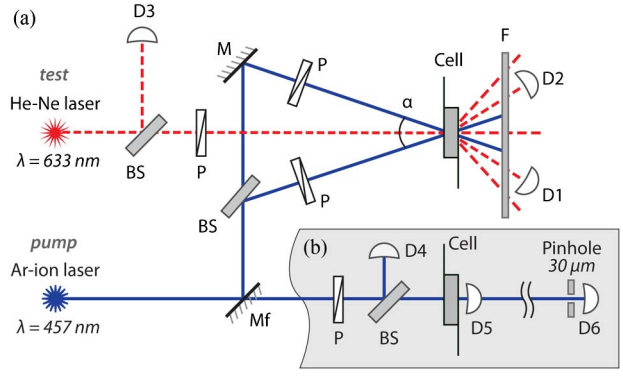

Fig. 3. (a) Experimental setup for grating recording: Mf, flip mirror; M, mirror; BS, beam splitters; P, polarizers; F, filter to cut recording beams; D1, D2, photodiodes for measuring diffracted beam intensities; D3, photodiode for measuring test beam incident intensity; α, angle between recording beams and (b) experimental setup for detecting of light-induced changes of the total and on-axis transmittances with one recording beam of Ar-ion laser: Mf is absent; D4, photodiode for measuring total intensity; D5, photodiode for measuring total transmittance just after the cell; D6, photodiode for measuring on-axis transmittance at a distance of 75 cm from the cell.

The cell's plane and the LC director were perpendicular to the incidence plane. The interference pattern in a cell's plane

$$I = I_0\left(1 + 2\frac{\sqrt{I_1 I_2}}{(I_1 + I_2)}\cos(2\pi x/\Lambda)\right) = I_0(1 + \cos(2\pi x/\Lambda)), \tag{1}$$

with a period of $\Lambda = \lambda_{\text{pump}}/2\sin(\alpha/2)$ (where x is the coordinate along the pattern and α is the angle between the recording beams), resulted in the recording of thin Raman–Nath type optical gratings. The Raman–Nath diffraction behavior was verified [12] via the Klein–Cook parameter [13] defined as $Q = 2\pi\lambda L/n\Lambda^2$, where λ is the vacuum wavelength, L is the thickness of the cell, n is the mean refractive index, and Λ is the grating period. Since Q was < 1 (0.5 for 10 μm grating period, 0.05 for 30 μm grating period, and 0.02 for 50 μm grating period), the recorded gratings were of the Raman–Nath type [12]. Both the intensities of the first self-diffraction orders of the pump Ar-ion laser beams $I_d^{\pm 1}$ and intensities of the first diffraction orders of the test beam of the He–Ne laser ($\lambda_{\text{test}} = 633$ nm), $I_{d,\text{test}}^{\pm 1}$, were measured as a function of the intensity, polarization, period of the interference pattern, and the exposure time. In the Raman–Nath regime, in a case of a very small amplitude and phase modulation, the diffraction efficiency η of the grating is connected with a change of the refractive index Δn by the formula

$$\eta = I_{d,\text{test}}^{\pm 1}/I_{\text{test}} = J_1^2(2\pi L\Delta n(I_0)/\lambda_{\text{test}}) \approx |\pi L\Delta n(I_0)/\lambda_{\text{test}}|^2, \tag{2}$$

where J_1 is the first-order Bessel function, L is the cell's thickness, and λ_{test} is the wavelength of the test beam.

B. Holographic Grating Recording

After switching on the recording beams, the diffracted beams appeared, and the diffraction efficiency η achieved a stationary value η_{sat} within several seconds. After switching off the recording beams, the gratings fully relaxed. The recorded gratings were fully reversible, and no residual diffraction was observed in the irradiated areas after numerous recording–relaxing cycles.

The stationary saturated value of the diffraction efficiency η_{sat} strongly depended on the polarization of the recording and test beams to the orientation of the LC director. The maximal self-diffraction and the diffraction of the test beam were observed when the polarization of the pump and test beams coincided with the LC director, which meant that an extraordinary wave (e-wave) was propagating in the LC (see Table 1; the angle α between the two recording beams was 0.87°, which corresponds to a grating period of $\Lambda = 30$ μm). Such polarization dependence is typical for LC systems with a light-induced isomerization of own or dopant molecules [14]. In these systems, the light-induced changes of the refractive index Δn are proportional to the concentration of the light-induced isomers, c, which is most effective for the extraordinary wave because of the positive absorption dichroism of the LC molecules and dopants. Thus, all the following measurements were done in the ee-e configuration, where the first indices denote the recording beams and the third index is for the test beam polarization.

Table 1. Number of Orders Observed in the Diffraction of the Test Beam and in the Self-Diffraction in Different Irradiation Geometries of the Complex-Doped LC

Geometry (Recording Beams–Test Beam Polarization)	Pump I_0, mW/cm^2	No. of Orders of Self-Diffraction	No. of Orders of Test Beam
oo-e	110	0	2
ee-e	110	3	3
ee-o	110	3	2
oo-o	110	0	1

Figure 4 shows the diffraction efficiency of the first-order diffraction of the test beam as a function of the intensity of the recording beams and grating period. The complex-doped LC appeared to be *twice* as effective as LC doped only with azo dye. The intensity dependence of the saturated stationary diffraction efficiency η_{sat} was not monotonic [Fig. 4(a)], but it had a maximum of nearly 0.25% for a range of intensities of 30–100 mW/cm^2. For larger intensities, the efficiency decreased and showed a tendency to saturation. As for dye-doped LC, the intensity dependence of diffraction efficiency was almost monotonic, contrary to the complex-doped LC, and saturates with intensity. Using the formula in Eq. (2) for the case of maximum diffraction efficiency, the refractive index change Δn and nonlinear parameter $n_2 = \Delta n/I_0$ of complex-doped LC can be obtained: $\Delta n \approx 5 \times 10^{-4}$, and n_2 is up to 10^{-2} cm^2/W.

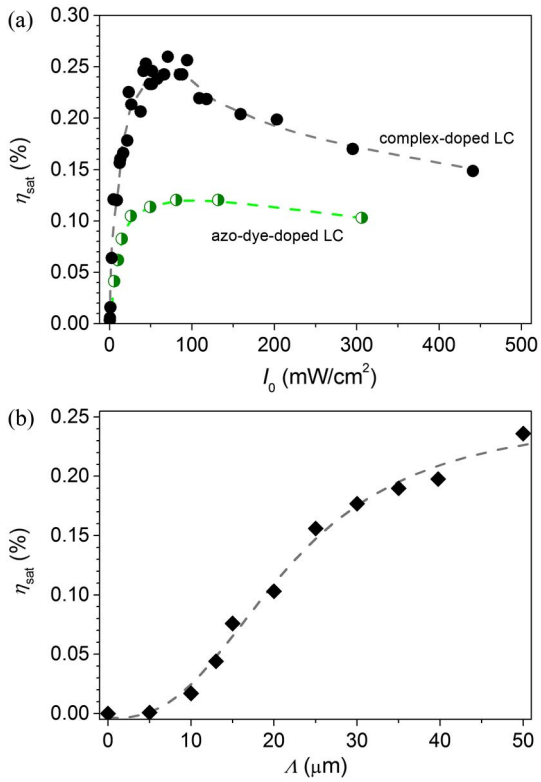

Fig. 4. (a) Dependence of the saturated stationary diffraction efficiency η_{sat} of the first-order diffraction of the test beam in the complex-doped and azo-dye-doped LC on intensity (the grating period is $\Lambda = 30$ μm). (b) Dependence of the stationary diffraction efficiency on the grating period (the total intensity $I_0 = 30$ mW/cm^2) in the complex-doped LC. The recording and test beams were parallel to the LC director (e-waves).

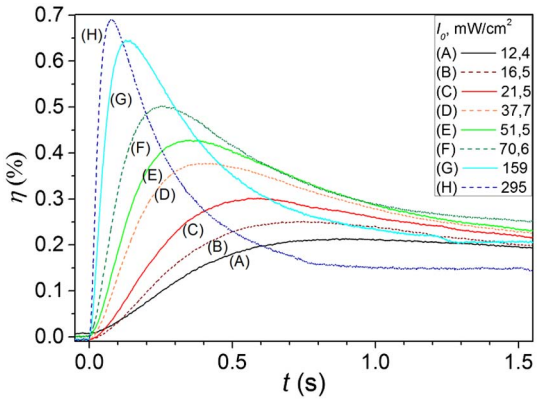

Fig. 5. Dynamics of the first-order diffraction efficiency at grating recording in the complex-doped LC. The grating period is $\Lambda = 30$ μm.

The dependence of the diffraction efficiency on the period of the grating is presented in Fig. 4(b). In the measured range, η_{sat} increased with the period Λ with a changing rate: faster up to $\Lambda = 30$ μm, and then slower beyond that.

The dynamics of the grating recording are unusual and strongly depend on the intensity of the recording beams (Fig. 5). The dependence $\eta(t)$ is monotonic at low intensities (< 20 mW/cm^2), and has an extremum at the high intensities. This maximum shifts to the shorter exposure times and becomes more pronounced with the increase of the intensity. We cannot claim that this extremum is caused by overmodulation, as even at high intensities, the observed maximal values of diffraction efficiency are far below the theoretically expected value of 33.8% for a thin phase grating, 6.25% for a sinusoidal transmittance grating [15,16], or 4.8% for a grating of modulation of absorbance [17].

1. Optical Bleaching and Defocusing

To understand the unusual dynamics of the gratings formation in the complex-doped LC (Fig. 5), we measured the dependence of the light-induced changes of the total (Fig. 6) and on-axis transmittances (Fig. 7) on the laser intensity at 457 nm using a method which is a modification of the spatial profile analysis technique [18]. Only one pump laser beam was used to irradiate the sample [Fig. 3(b)]. Since, during the grating recording, the intensity modulation in the cell's plane is $I = I_0(1 + \cos(2\pi x/\Lambda))$, i.e., the intensity at the maximum is $2I_0$, we applied a one-beam intensity of $I_{pump} = 2I_0$ to have the same effect on the sample. The laser beam was not convergent/divergent, and the beam waist at the sample plane was about 1 mm. The spot was stable over the time of the experiment. A set of photodiodes [Fig. 3(b)] measured incident laser power (before the sample), the total transmitted power through the sample (close after the sample), and the on-axis transmittance through a pinhole (30 μm) in the far field, visualizing the light-induced convergence/divergence of the beam, if any. All dependences were normalized to the spectral transmittance at 457 nm before the irradiation in order to distinguish the nonlinear optical response.

The experiments showed an increase of the sample's transmittance by a factor of more than two, and the dependence on the intensity [Fig. 6(a)]. This is assumed to be due to optical bleaching, i.e., light-induced change of the absorption coefficient, which strongly depends on the intensity [Fig. 6(b)].

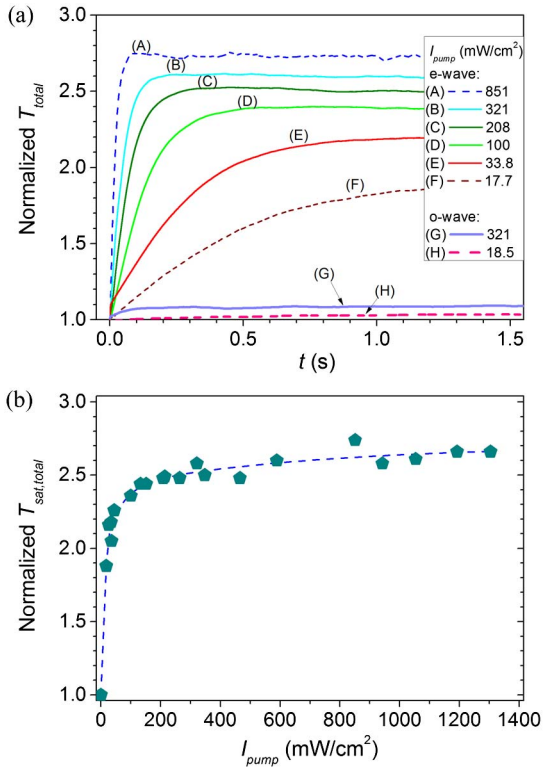

Fig. 6. (a) Dynamics of the normalized total transmittance T_{total} of the complex-doped LC irradiated with e and o waves and (b) dependence of the saturated value $T_{sat,total}$ on intensity at e-wave irradiation. The transmittances were normalized to the spectral transmittance at 457 nm before irradiation.

The dynamics of the on-axis transmittance of the sample measured through a pinhole in the far field [Fig. 7(a)] showed defocusing, i.e., light-induced refractive index change occurred. Light-induced defocusing depended on intensity [Fig. 7(b)]. The defocusing is quite strong (up to 45% at high intensities), and can be clearly seen when the refractive nonlinear response is separated from the absorptive one by normalizing of the on-axis transmittance to total transmittance [Fig. 7(c)]. At low intensities, the defocusing effect diminishes and disappeared at intensities < 100 mW/cm^2. In the dye-doped LC, the light-induced defocusing is lower compared with complex-doped LC, and does not exceed 9%. To prove the appearance of defocusing effect, we measured the Gaussian profile of the laser beam without and with the cell using the knife-edge technique [19] at distances right after the cell and in the far field. The measured profiles showed that, in the far field after the cell, the Gaussian beam waist increased with distance. These results confirmed light-induced defocusing.

At irradiation of the complex-doped LC, there are thus observed both a light-induced change of the absorption coefficient, causing optical bleaching, and a light-induced change of the refractive index causing beam defocusing. Obviously, the same processes occur at the grating recording. The holographic gratings appeared to be formed by a light-induced change of both the absorption coefficient and the refractive index. These processes depend on intensity.

C. Holographic Grating Relaxation

The relaxation of the gratings is also unusual. The relaxation process was measured by tracking the intensity of a test beam

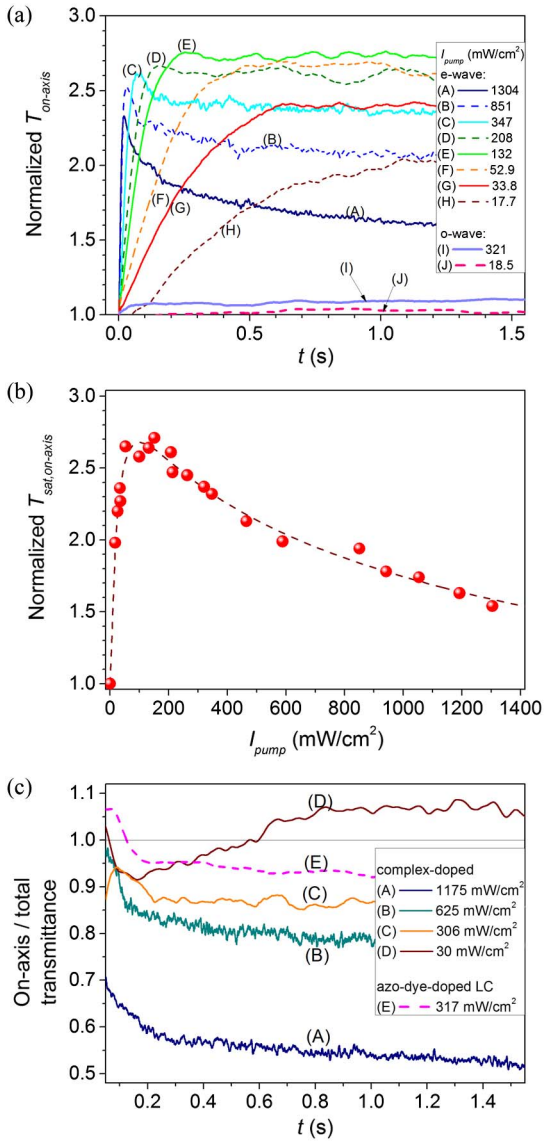

Fig. 7. (a) Dynamics of the normalized on-axis transmittance $T_{\text{on-axis}}$ of the complex-doped LC irradiated with e and o waves ($T_{\text{on-axis}}$ normalized to the spectral transmittance at 457 nm before irradiation). (b) Value of the normalized on-axis transmittance after saturation $T_{\text{sat,on-axis}}$ versus pump intensity. (c) Dynamics of the normalized on-axis to total transmittance of the complex-doped and azo-dye-doped LCs.

using a photodiode connected to an oscilloscope as the recording beams were switched off. It appeared that the relaxation process could not be fitted with a single exponential function, but that was well described with two exponentials $A_1e^{-t/\tau_1} + A_2e^{-t/\tau_2}$, giving two characteristic relaxation times τ_1 and τ_2 (Fig. 8). Moreover, both relaxation times depended on the intensity of the recording beams [Fig. 8(b)]. The amplitudes were $A_1/A_2 > 1$ and also depended on the intensity. Both relaxation times for the complex-doped LC were almost twice longer than those for the LC doped with the same azo dye only.

To understand the origin of the grating relaxation, we measured the thermal relaxation rate of the *cis* isomer of the azo dye in the complex-doped LC using the method of Barrett *et al.* [20]. Exciting the chromophores with a circularly polarized

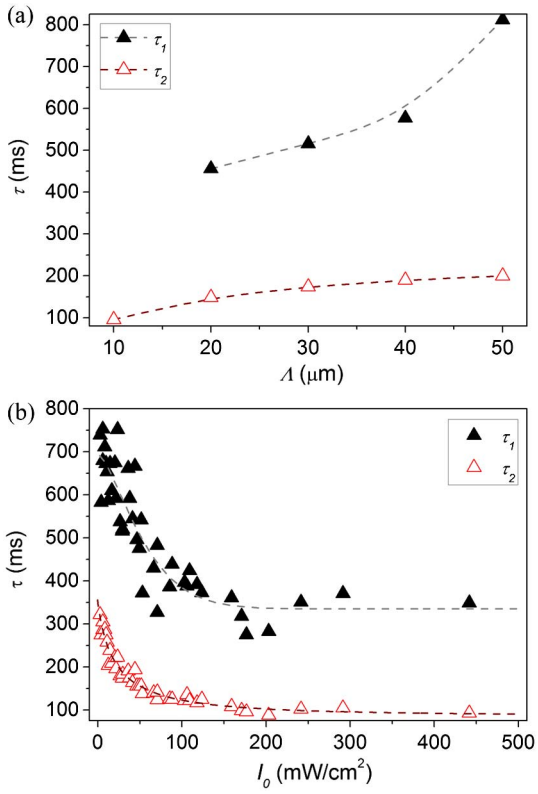

Fig. 8. Dependence of the grating relaxation in the complex-doped LC: (a) on the period (the total intensity $I_0 = 30$ mW/cm^2) and (b) on the total intensity of the recording beams (grating period is $\Lambda = 30$ μm). The recording and test beam polarizations were parallel to the LC director (e-waves).

pump beam ($\lambda = 457$ nm, 30 mW/cm^2, Xenon-arc lamp filtered with a bandpass filter at 470 nm) for 4 s and detecting with an Ocean Optics HR4000CG-UV-NIR spectrometer the subsequent transmittance caused by *cis-trans* isomerization gave the half-lifetime τ_{cis} for the HAB–DMA *cis* isomer in the complex in LC (530 ms). The half-lifetime obtained here correlates well with one of the grating relaxation times τ_1 [Fig. 8(b)], thus indicating that one of the relaxation mechanisms is the thermal *cis*-to-*trans* isomerization of the azobenzene molecules. The half-lifetime of the dye *cis* isomer without H bonding was shorter. The hydrogen bonding between the hydroxyl group from the azo dye and the pyridine nitrogen from the polymer seems to stabilize the *cis* form of the azo dye, making the thermal relaxation slower.

4. DISCUSSION

As we expected, the optical nonlinearity in the complex-doped LC was enhanced (the nonlinear parameter was up to 10^{-2} cm^2/W), and thus recording of the holographic gratings appeared to be more effective than in LC doped with the same azo dye only. The presence of the polymer and its connection with the azo dye molecules via H bonds definitely makes a difference; it results in a change of the optical properties, which improves the efficiency of the holographic grating by a factor of two. This improvement has several reasons. First, the complex unit is much heavier than a separate azo dye molecule, making the diffusion process slower, thus, the light impact at grating recording is more effective. Second,

the *cis* form of the azo dye in a complex lives longer, making the system more stable. Third, the polymer–azo-dye complex in the LC provides structural changes in the nematic matrix compared to the azo-dye-doped LC: the LC molecules now have a different symmetry in their arrangement with respect to the azo dye, which is bound to the polymer chain. In a dye-doped LC, the azo dye molecules are "free" and surrounded by LC molecules from all around; in the case of the complex, the azo dye molecules are only partially surrounded by LC molecules due to the presence of polymer chain. In [21], the authors suggest that in the nonlinearity mechanism, this difference in molecule arrangement plays an important role: during orientation-selective excitation of molecules (which are dichroic) by polarized light, there is a torque due to changes in intermolecular forces before and at irradiation. This torque is different for "free" dye molecules and H-bonded ones. Thus at irradiation, the interaction of H-bonded azo dye molecules and LC matrix is different from the interaction of "free" molecules and LC ones, and the influence on order parameter change or dye-assisted LC reorientation will be different in dye-doped and complex-doped LCs.

All previously mentioned changes in the complex-doped LCs result in double effective grating. In the following section, we qualitatively discuss the grating formation/relaxation and its anomalies in the complex-doped LC in detail.

A. Light-Induced Changes in the Complex-Doped LC

In general, to explain the behavior of the complex-doped LC under irradiation with resonant light, one should refer to the characteristics of the azo dye in the composite. Many azobenzene compounds undergo the *trans*-to-*cis* photoisomerization process either in solution [22] or in liquid-crystalline solid matrices [23]. Azobenzene molecules have two stable configurations or isomers: the *trans* isomer, with a planar conformation of the aromatic rings together with the azo group (rod-like shape), and the *cis* isomer, with an out-of-plane configuration of the aromatic rings (bend-like shape). The *trans*-to-*cis* isomerization process will take place when irradiating the *trans* isomer with resonant light, while the *cis* isomer can be isomerized either by means of light or heat. The *trans* isomer usually has two main absorption bands which correspond to the $n-\pi^*$ electronic transition ($S_1 \leftarrow S_0$) and the $\pi-\pi^*$ electronic transition ($S_2 \leftarrow S_0$), while the *cis* isomer has the same transitions shifted to shorter wavelengths [24].

The HAB–DMA dye molecule is an aminoazobenzene-type derivative with an amino electron donor group in the *para* position (dimethylamino) with a $\pi-\pi^*$ electronic transition band shifted to longer wavelengths. The $\pi-\pi^*$ band overlaps with the $n-\pi^*$ electronic transition band and aids the photoisomerization process. The absorption of a photon at $\lambda_{\text{pump}} = 457$ nm by the *trans* isomer promotes an excitation of one electron from the occupied π bonding (π) or the nonbonding (n) molecular orbital to the empty π antibonding molecular orbital (π^*) in time scales of the order of 1–10 ps [25]. Then, the excited *trans* isomer undergoes a transformation into an excited *cis* isomer state in the π antibonding molecular orbital (π^*), which relaxes to its corresponding ground state through an adiabatic photoreaction [26]. The final ground *cis* isomer state evolves upon time to the corresponding ground *trans* isomer state due to the low activation energy barrier, closing the cycle in less than a second.

Figure 9 shows two main absorption bands of the complex-doped LC S_1 and S_2 at $\lambda_{n-\pi^*} = 456$ nm and at $\lambda_{\pi-\pi^*} = 412$ nm for the *trans* isomer. After conversion to the *cis* isomer, the absorption bands shift to $\lambda_{n-\pi^*} = 448$ nm and $\lambda_{\pi-\pi^*} = 367$ nm. The analysis of the spectrum at irradiation shows the absorption bands due to the presence of a residual amount of the *trans* isomers, and allows for the estimation of a concentration of the *cis* isomers of approximately 70%.

When the azo dye molecule isomerizes, it changes the transmittance of the system and induces reorientation of either the LC director [3,4] or a local disorder of the liquid–crystalline matrix [1], that leads to a change in the intrinsic refractive/absorption parameters of the whole system. We have calculated order parameter change [8] based on the polarization spectra of the complex-doped LC without and with irradiation using the formula

$$S_{\text{LC}} \approx S_{\text{dye}} = (A_{\text{max},||} - A_{\text{max},\perp})/(A_{\text{max},||} + 2A_{\text{max},\perp}), \quad (3)$$

where $A_{\text{max},||}$ and $A_{\text{max},\perp}$ are the absorption maxima for light polarized parallel and perpendicular to the LC director, respectively (Fig. 2). We observed a decrease of the order parameter from $S = 0.43$ to 0.26 at irradiation with an e-wave of intensity 300 mW/cm^2 at 457 nm. Based on the polarization spectra (Fig. 2) and the fact that the grating recording in the complex-doped LC is the most effective in the ee-e irradiation configuration, the dye-assisted reorientation mechanism can be neglected. Thus, light-induced order parameter change due to the *trans*-to-*cis* photoisomerization process of the

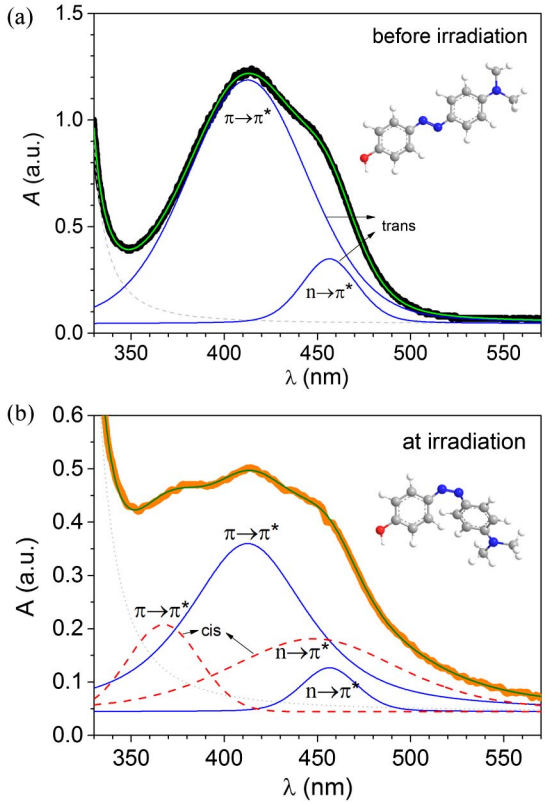

Fig. 9. UV–Vis deconvoluted spectra of the complex P4VP(HAB–DMA)$_{0.5}$ in the 5CB matrix (a) before irradiation and (b) at irradiation with e-wave of 457 nm laser of 300 mW/cm^2. The thickness of the cells was 20 μm.

azo dye molecules in the complex is responsible for the grating formation in the complex-doped LC.

B. Anomalies in Holographic Grating Formation/Relaxation

The following peculiarities in the behavior of the holographic gratings in the complex-doped LC were observed:

- the grating relaxation process, which is described with the sum of exponentials with two characteristic times [Figs. 8(a) and 8(b)];
- intensity dependence of two grating relaxation times [Fig. 8(b)];
- nonmonotonic dependence of the saturated stationary diffraction efficiency η_{sat} on the total intensity of the recording beams [Fig. 4(a)];
- dependence of the dynamic behavior of the diffraction efficiency $\eta(t)$ on the total intensity of the recording beams (Fig. 5);
- light-induced change of both refractive index and absorption coefficient, which depend on time and intensity differently (Figs. 6 and 7).

All these pecularities cannot be explained by the conventional model usually used in a case of grating recording in dye-doped LCs [1,14]. This model assumes that grating recording is caused by an isomerization of the photosensitive molecules, and the light-induced change in the refractive index Δn is proportional to the isomer concentration, namely, number of phototransformed molecules [1,14]. The isomer concentration, in its turn, is proportional to the total intensity of the recording beams I_0 [14]. From Eq. (2) $\eta \sim \Delta n^2$, the diffraction efficiency is proportional to the isomer concentration, and thus to the total intensity. In the framework of this model, $\eta(I_0)$ should be quadratic at small intensities and saturate when reaching the photostationary equilibrium or maximum *cis* isomer concentration at high intensities. On the contrary, the experimentally obtained dependence $\eta(I_0)$ is not monotonic [Fig. 4(a)], but has an extremum.

The dynamics of the grating formation/relaxation also cannot be explained by a simple model of the photoisomerization of the dopants, in which these processes are described by a single exponential function with the characteristic time determined by the diffusion of the isomers and their lifetime. Thus, the multiple relaxation model should be suggested.

1. Two Relaxation Times

Despite the fact that it has not been seen on all azo dyes [1,9,11], multiple relaxation pathways [24] of *cis* isomers following $S_1 \leftarrow S_0$ excitation have been predicted by simulations [27]. Similar to what we observed in the complex-doped LC, it has been seen that direct $S_1 \leftarrow S_0$ excitation can relax not only monomodally, but bimodally or even stretched exponentially [28,29], depending on the solvent viscosity [30] and excitation wavelength [31,32]. Using a three-state model for photoisomerization and assuming the optical transition rate from the *trans*-to-trans* state and the thermal relaxation rate from *cis*-to-*trans* states to have a form of the stretched exponential (or biexponential, as in our case), the authors of Ref. [29] were able to analyze and explain the nonmonotonic behavior of the diffraction efficiency and the photoinduced birefringence. In this analysis, the concentration of the isomers depended on the relaxation time and the degree of its dispersion through the expression [29]

$$c \sim \frac{S(x)}{1+S(x)}\left[1-\exp\left\{-(1+S(x))\left(\frac{t}{\tau}\right)^{\beta}\right\}\right]. \tag{4}$$

Here, $S(x) = I(x)/I_{sat}$ is a saturation parameter, where $I_{sat} \sim \tau^{-1}$ is the saturation intensity for the holographic grating, τ is the azo molecules' characteristic time, and $I(x)$, given by Eq. (1), is the intensity interference pattern. The parameter β $(0 < \beta < 1)$ is a stretched exponent which quantifies the extent of the deviation from pure exponential, meaning that there is a dispersion of relaxation times [28]. In other words, the process of relaxation can be described with a set of exponents.

Assuming that the relaxation of the *cis* isomers occurs through different pathways (rotation, inversion, etc. [24]), one can get two (at least) characteristic times describing relaxation of the gratings. The slower component of the grating relaxation process in the complex-doped LC with τ_1 is more pronounced while the amplitude of the fast relaxation component with τ_2 is smaller. The reason why the fast component has not been seen at half-lifetime measurements of *cis* isomer is still under discussion.

2. Grating Relaxation versus Intensity

The dependence of the grating relaxation times on intensity can be explained as follows. As was shown in [33], the order parameter S of the LC doped with an additive, which can undergo conformational changes, depends on the concentration of the transformed molecules of the dopant. With the increase of the pump intensity, the amount of the *cis* isomer molecules grows, reducing order parameter [see calculation with Eq. (3) in Section 4.A] and inducing the LC matrix state closer to the isotropic phase [33]. Since the matrix environment changes with intensity, the half-lifetime of the *cis*-form molecules τ_{cis} also changes depending on the order parameter of the LC [34]. As the relaxation time of the grating τ is determined by the half-lifetime of the *cis*-form molecules τ_{cis} (see Section 3.C), the higher the intensity, the lower the order parameter, and consequently the faster the relaxation time of the grating, which was experimentally observed.

3. Grating Diffraction Efficiency

Having two relaxation times, the nonmonotonic behavior of the saturated stationary $\eta_{sat}(I)$ [Fig. 4(a)] can easily be explained. Since diffraction efficiency is proportional to *cis* isomer concentration, η also depends on two characteristic times and on the saturation parameter $S(x)$ [Eq. (4)], which in turn depends on these characteristic times, thus making the dependence nonmonotonic.

4. Nonlinear Absorptive/Refractive Response

The optical bleaching caused by light-induced change of the absorption coefficient and the light-induced beam defocusing caused by light-induced change in the order parameter, and thus in the effective refractive index, are the two mechanisms suggested to be responsible for the dynamics of the holographic gratings in the complex-doped LC. In contrast to the conventional gratings in azo-dye-doped LCs [1,2], where usually only a phase grating is recorded due to a change of

the refractive index, in our complex-doped LC, both absorption coefficient and refractive index changes are involved, i.e., both amplitude and phase gratings are recorded. Both absorption coefficient and refractive index changes are caused by photoisomerization, but the change in the absorption coefficient is connected with the dye while the change of the refractive index is determined with the LC matrix perturbation due to dye form change. These two mechanisms dominate at different time and intensity ranges. In the beginning, the light-induced absorption dominates, but with time, the light-induced refractive nonlinear response starts to gain at intensities $>100\ \mathrm{mW/cm^2}$. Both processes depend on the intensity, so that the grating development will show a nonmonotonic behavior (Fig. 5).

To summarize, all the observed anomalies of the optical properties of the studied system can be explained by different symmetry in the arrangement of the LC molecules with respect to the azo dye bounded to the polymer side fragment, dispersion of the relaxations of the *cis* isomers in the presence of the polymer with H bonds, and modulation of both the absorption coefficient and the refractive index of the system. The doping of LC with polymer–azo-dye complex leads to the enhancement of optical nonlinearity of LC: at the same experimental conditions, there is no grating formation in LC or polymer-doped LC, but the holographic grating in complex-doped LC is twice as efficient as in LC doped with the same amount of free azo dye.

5. CONCLUSIONS

We observed the enhancement of optical nonlinearity with high nonlinear parameter (up to $10^{-2}\ \mathrm{cm^2/W}$) in a new heterogeneous liquid-crystalline material where a H-bonded polymer–azo-dye complex was used as a dopant in a LC bulk matrix at low concentration. The effective dynamic holographic gratings were recorded in the complex-doped LC. Double enhancement of the diffraction efficiency of holographic gratings recorded in the complex-doped LC, compared to a plain azo-dye-doped LC with the same dye, was observed at very low intensities (of an order of tens of $\mathrm{mW/cm^2}$). Moreover, the grating formation/relaxation processes in complex-doped LC showed anomalies: nonmonotonic intensity dependence of the stationary and dynamic diffraction efficiency of the first-order diffraction, and two characteristic times describing the grating relaxation process depending on intensity. The observed peculiarities in the optical properties of the complex-doped LC were explained by different symmetry in the arrangement of the LC molecules with respect to the azo dye bounded to the polymer, temporal dispersion of the relaxations of the *cis* isomers in the presence of the polymer with H bonds that provides limited mobility of the azo dye molecules, and modulation of both the absorption coefficient and the refractive index due to *trans*-to-*cis* photoisomerization. The observed enhancement of nonlinearity by H-bonded polymer–dye complexes as dopants in LC gives perspectives for new ways of control and tuning of the LC properties and novel optical applications.

ACKNOWLEDGMENTS

This research was supported by the Academy of Finland (PHORMAT project no. 135106). We are grateful to Prof. Yu. Reznikov (Institute of Physics, NAS of Ukraine), Dr. V. Gaivoronsky (Institute of Physics, NAS of Ukraine), and Dr. A. Shevchenko (Aalto University, Finland) for useful discussions.

REFERENCES

1. I. P. Pinkevich, Yu. A. Reznikov, V. Yu. Reshetnyak, and O. V. Yaroshchuk, "Conformational optical nonlinearity of nematic liquid crystals," Int. J. Nonlinear Opt. Phys. **1**, 447–472 (1992).
2. I. C. Khoo, P. H. Chen, M. Y. Shih, A. Shishido, S. Slussarenko, and M. V. Wood, "Supra optical nonlinearities of methyl-red and azobenzene liquid crystal-doped nematic liquid crystals," Mol. Cryst. Liq. Cryst. **358**, 1–13 (2001).
3. I. A. Budagovsky, A. S. Zolot'ko, V. N. Ochkin, M. P. Smayev, S. A. Shvetsov, A. Yu. Bobrovsky, N. I. Boiko, V. P. Shibaev, and M. I. Barnik, "Orientational optical nonlinearity of nematic liquid crystals induced by high-molecular-mass azo-containing compounds," Polym. Sci. Ser. A **53**, 655–665 (2011).
4. A. S. Zolot'ko, I. A. Budagovsky, V. N. Ochkin, M. P. Smayev, A. Yu. Bobrovsky, V. P. Shibaev, N. I. Boiko, A. I. Lysachkov, and M. I. Barnik, "Light-induced director reorientation in nematic liquid crystals doped with azobenzene-containing macromolecules of different architecture," Mol. Cryst. Liq. Cryst. **488**, 265–278 (2008).
5. L. Lucchetti, M. Gentili, F. Simoni, S. Pavliuchenko, S. Subota, and V. Reshetnyak, "Surface-induced nonlinearities of liquid crystals driven by an electric field," Phys. Rev. E **78**, 061706 (2008).
6. L. Lucchetti and F. Simoni, "Role of space charges on light-induced effects in nematic liquid crystals doped by methyl red," Phys. Rev. E **89**, 032507 (2014).
7. E. A. Babayan, I. A. Budagovsky, S. A. Shvetsov, M. P. Smayev, A. S. Zolot'ko, N. I. Boiko, and M. I. Barnik, "Light- and electric-field-induced first-order orientation transitions in a dendrimer-doped nematic liquid crystal," Phys. Rev. E **82**, 061705 (2010).
8. E. Ouskova, J. Vapaavuori, and M. Kaivola, "Self-orienting liquid crystal doped with polymer-azo-dye complex," Opt. Mater. Express **1**, 1463–1470 (2011).
9. E. Ouskova and M. Kaivola, "Nonlinear optical response of self-orienting liquid crystal," Opt. Mater. Express **2**, 1056–1063 (2012).
10. A. V. Uklein, A. A. Vasko, E. V. Ouskova, M. S. Brodyn, and V. Ya. Gayvoronsky, "Nonlinear optical properties of new photosensitive smart materials based on nematic liquid crystal with H-bonded dye-polymer complex," Opt. Commun. **296**, 79–83 (2013).
11. J. Vapaavuori, V. Valtavirta, T. Alasaarela, J.-I. Mamiya, A. Priimagi, A. Shishido, and M. Kaivola, "Efficient surface structuring and photoalignment of supramolecular polymer–azobenzene complexes through rational chromophore design," J. Mater. Chem. **21**, 15437–15441 (2011).
12. M. G. Moharam, T. K. Gaylord, and R. Magnusson, "Criteria for Raman–Nath regime diffraction by phase gratings," Opt. Commun. **32**, 19–23 (1980).
13. W. R. Klein and B. D. Cook, "Unified approach to ultrasonic light diffraction," IEEE Trans. Sonics Ultrason. **14**, 123–134 (1967).
14. S. G. Odulov, Yu. A. Reznikov, M. S. Soskin, and A. I. Khizhnyak, "Photostimulated transformation of molecules—a new type of "giant" optical nonlinearity in liquid crystals," Zh. Eksp. Teor. Fiz. **82**, 1475 (1982) [Sov. Phys. JETP 55, 854 (1982)].
15. P. Hariharan, *Optical Holography: Principles, Techniques, and Applications*, 2nd ed. (Cambridge University, 1996).
16. R. J. Collier, C. B. Burkhardt, and L. H. Lin, *Optical Holography* (Academic, 1971), Section 8.5.
17. L. Song, R. A. Lessard, and P. Galarneau, "Diffraction efficiency of a thin amplitude-phase holographic grating: a convolution approach," J. Mod. Opt. **37**, 1319–1328 (1990).
18. V. Gayvoronsky, S. Yakunin, V. Nazarenko, V. Starkov, and M. Brodyn, "Techniques to characterize the nonlinear optical response of doped nematic liquid crystals," Mol. Cryst. Liq. Cryst. **426**, 231–241 (2005).
19. M. A. de Araújo, R. Silva, E. de Lima, D. P. Pereira, and P. C. de Oliveira, "Measurement of Gaussian laser beam radius using the knife-edge technique: improvement on data analysis," Appl. Opt. **48**, 393–396 (2009).

20. C. Barrett, A. Natansohn, and P. Rochon, "Cis-trans thermal isomerization rates of bound and doped azobenzenes in a series of polymers," Chem. Mater. **7**, 899–903 (1995).
21. I. A. Budagovsky, A. S. Zolot'ko, V. N. Ochkin, M. P. Smayev, A. Yu. Bobrovsky, V. P. Shibaev, and M. I. Barnik, "Orientational optical nonlinearity induced by comb-shaped polymers in a nematic liquid crystal," J. Exp. Theor. Phys. **106**, 172–181 (2008).
22. W. R. Brode, J. H. Gould, and G. M. Wyman, "The relation between the absorption spectra and the chemical constitution of dyes XXV. Phototropism and cis-trans isomerism in aromatic azo compounds," J. Am. Chem. Soc. **74**, 4641–4646 (1952).
23. A. Sánchez-Ferrer, A. Merekalov, and H. Finkelmann, "Opto-mechanical effect in photoactive nematic side-chain liquid-crystalline elastomers," Macromol. Rapid Commun. **32**, 672–678 (2011).
24. H. M. D. Bandara and S. C. Burdette, "Photoisomerization in different classes of azobenzene," Chem. Soc. Rev. **41**, 1809–1825 (2012).
25. S. G. Mayer, C. L. Thomsen, M. P. Philpott, and P. J. Reid, "The solvent-dependent isomerization dynamics of 4-(Dimethylamino)azobenzene (DMAAB) studied by subpicosecond pump-probe spectroscopy," Chem. Phys. Lett. **314**, 246–254 (1999).
26. H. Dürr and H. Bouas-Laurent, *Photochromism: Molecules and Systems* (Elsevier Science, 2003).
27. G. Granucci and M. Persico, "Excited state dynamics with the direct trajectory surface hopping method: azobenzene and its derivatives as a case study," Theor. Chem. Acc. **117**, 1131–1143 (2007).
28. M. Knežević, M. Warner, M. Čopič, and A. Sánchez-Ferrer, "Photodynamics of stress in clamped nematic elastomers," Phys. Rev. E **87**, 062503 (2013).
29. C. H. Kwak and H. R. Yang, "Determinations of optical field induced nonlinearities in azo dye doped polymer film," in *Polymer Thin Films*, A. A. Hashim, ed. (InTech, 2010), pp. 309–324.
30. T. Fujino and T. Tahara, "Picosecond time-resolved Raman study of trans-azobenzene," J. Phys. Chem. A **104**, 4203–4210 (2000).
31. C.-W. Chang, Y.-C. Lu, T.-T. Wang, and E. W.-G. Diau, "Photoisomerization dynamics of azobenzene in solution with S1 excitation: a femtosecond fluorescence anisotropy study," J. Am. Chem. Soc. **126**, 10109–10118 (2004).
32. I. K. Lednev, T. Q. Ye, P. Matousek, M. Towrie, P. Foggi, F. V. R. Neuwahl, S. Umapathy, R. E. Hester, and J. N. Moore, "Femtosecond time-resolved UV-visible absorption spectroscopy of trans-azobenzene: dependence on excitation wavelength," Chem. Phys. Lett. **290**, 68–74 (1998).
33. S. G. Odulov, Yu. A. Reznikov, M. S. Soskin, and A. I. Khizhnyak, "Photostimulated change of phase-transition temperature and "giant" optical nonlinearity of liquid crystals," Sov. Phys. JETP **58**, 1154 (1983).
34. D. Statman and I. Janossy, "Study of photoisomerization of azo dyes in liquid crystals," J. Chem. Phys. **118**, 3222–3232 (2003).